iPLA$_2$, a novel determinant in Ca^{2+}- and phosphorylation-dependent S100A8/A9 regulated NOX2 activity

Véronique Schenten [a], Sabrina Bréchard [a], Sébastien Plançon [a], Chantal Melchior [a], Jean-Pol Frippiat [b], Eric J. Tschirhart [a,*]

[a] *Life Sciences Research Unit, University of Luxembourg, 162A Avenue de la Faïencerie, L-1511 Luxembourg*
[b] *JE 2537, Development and Immunogenetics, Nancy-University, Vandœuvre-lès-Nancy, France*

ARTICLE INFO

ABSTRACT

The neutrophil NADPH oxidase (NOX2) is a key enzyme responsible for host defense against invading pathogens, via the production of reactive oxygen species. Dysfunction of NOX2 can contribute to inflammatory processes, which could lead to the development of diseases such as atherosclerosis. In this paper, we characterize a pathway leading to NOX2 activation in which iPLA$_2$-regulated p38 MAPK activity is a key regulator of S100A8/A9 translocation via S100A9 phosphorylation. Studies in cell-free or recombinant systems involved two Ca^{2+}-binding proteins of the S100 family, namely S100A8 and S100A9, in NOX2 activation dependent on intracellular Ca^{2+} concentration ([Ca^{2+}]$_i$) elevation. Using differentiated HL-60 cells as a model of neutrophils, we provide evidence that [Ca^{2+}]$_i$-regulated S100A8/A9 translocation is mediated by an increase in [Ca^{2+}]$_i$ through intracellular Ca^{2+} store depletion. Moreover, we confirm that p38 MAPK induces S100A9 phosphorylation, a mandatory precondition for S100 translocation. Based on a pharmacological approach and an siRNA strategy, we identify iPLA$_2$ as a new molecular player aiding S100 translocation and NOX2 activity. Inhibition of p38 MAPK activity and S100A9 phosphorylation by bromoenol lactone, a selective inhibitor of iPLA$_2$, indicated that p38 MAPK-mediated S100A9 phosphorylation is dependent on iPLA$_2$. In conclusion, we have characterized a pathway leading to NOX2 activation in which iPLA$_2$-regulated p38 MAPK activity is a key regulator of S100A8/A9 translocation via S100A9 phosphorylation.

© 2010 Elsevier B.V. All rights reserved.

1. Introduction

Neutrophils play an important role in defending their hosts against microbial pathogens by generating reactive oxygen species through the multicomponent enzyme NADPH oxidase (NOX2). Under pathophysiological conditions, NOX2 activity can persist at a high level. The large production of reactive oxygen species can cause tissue injury, potentially leading to the development of inflammatory diseases such as atherosclerosis or rheumatoid arthritis [1,2]. NOX2 activity has been shown to be regulated by intracellular Ca^{2+} concentration ([Ca^{2+}]$_i$) increase [3,4]. In neutrophils, the elevation of [Ca^{2+}]$_i$ is primarily due to intracellular Ca^{2+} store depletion-mediated Ca^{2+} influx [5]. Recently, S100A8 and S100A9, two members of the S100 family of Ca^{2+}-binding proteins [6] have been proposed as Ca^{2+}-dependent regulators of NOX2

activity [7–10]. S100A8 and S100A9 are able to form Ca^{2+}-dependent heterodimers and heterotetramers [11–13], the latter being probably the biologically active form in myeloid cells [14]. However, the precise link between [Ca^{2+}]$_i$ elevation, S100A8/A9 and regulation of NOX2 activity was not clearly delineated in a cellular model.

Since S100A8 and S100A9 are secreted upon stimulation [15], numerous extracellular functions have been attributed to these proteins, in particular, the mediation of neutrophil adhesion to fibronectin [16] and the induction of neutrophil chemotaxis [17]. Also, because S100A8 and S100A9 are up-regulated in diseases such as bronchitis, cystic fibrosis, rheumatoid arthritis and Crohn's disease, these proteins are largely used as markers of inflammation [18,19]. In addition to their extracellular functions, S100A8 and S100A9 are also involved in intracellular signaling pathways. The relevant role for S100A8/A9 complex has been established in NOX2 activation and is probably mediated via its translocation to the plasma membrane. Further, it has been suggested that the S100A8/A9 complex migrates from the cytosol to membrane structures and intermediate filaments in a Ca^{2+}-dependent fashion, which has been correlated to phagocytic activation [20–22].

However, several studies have revealed that Ca^{2+} concentration is probably not the sole factor controlling the regulation of S100A8/A9

migration. For example, the work of Lominadze et al. [23] demonstrated that S100A9 translocated at the base of lamellipodia after stimulation by the bacterial chemopeptide fMLF. Lominadze et al. [23] also demonstrated that this translocation was dependent on S100A9 phosphorylation. In addition, research has revealed that S100A9 phosphorylation is mediated by p38 MAPK [23,24] and that p38 MAPK can be activated in neutrophils [25]. Beckett et al. [26] showed that p38 MAPK activity could be altered by Ca^{2+}-independent phospholipase A_2 ($iPLA_2$) in ventricular myocytes. The hypothesis that $iPLA_2$ contributes to S100A9 phosphorylation and subsequent S100A8/A9 complex translocation to the cell membrane, has not yet been explored.

The aim of the present study is to characterize the regulatory pathways leading to S100A8/A9 translocation and subsequent regulation of NOX2 activation in differentiated HL-60 cells (dHL-60 cells), a model of neutrophils. Our data confirm that S100A9 phosphorylation and $[Ca^{2+}]_i$ changes are two events required for S100A8/A9 translocation. In addition, we provide evidence that $[Ca^{2+}]_i$ elevation-regulated S100A8/A9 translocation is triggered by Ca^{2+} release from internal stores. In addition, we demonstrate that both p38 MAPK and $iPLA_2$ are involved in S100A9 phosphorylation and that activation of p38 MAPK occurs downstream of $iPLA_2$ activation. Finally, we establish for the first time that $iPLA_2$ is an essential regulator of S100A8/A9 translocation-dependent NOX2 activity.

2. Materials and methods

2.1. Materials

The RPMI-1640 medium, fetal bovine serum, L-glutamine, penicillin and streptomycin were purchased from Lonza (Verviers, Belgium). N-formyl-L-Methionyl-L-Leucyl-L-Phenylalanine (fMLF), phorbol 12-myristoyl 13-acetate (PMA), thapsigargin, ethylene glycol-bis (beta-aminoethyl ether) N, N, N′, N′-tetraacetic acid (EGTA), ionomycin, DMSO, horseradish peroxidase (HRP) type II, SB203580, bromoenol lactone (BEL) and genistein were obtained from Sigma-Aldrich (Bornem, Belgium). Fura-2 acetoxymethylester (fura-2-AM), 10-acetyl-3,7-dihydroxyphenoxazine (Amplex Red) and 1,2-bis(o-aminophenoxy)ethane-N, N, N′, N′-tetraacetic acid acetoxymethylester (BAPTA-AM) were obtained from Invitrogen (Merelbeke, Belgium). All other chemicals were of analytical grade and obtained from Merck (Darmstadt, Germany). The physiological salt solution (PSS) used had the following composition: NaCl 115 mM, KCl 5 mM, KH_2PO_4 1 mM, glucose 10 mM, $MgSO_4$ 1 mM, $CaCl_2$ 1.25 mM, HEPES-Na 25 mM, which was supplemented with bovine serum albumin (BSA) 0.1% w/v, pH 7.4.

2.2. Cell culture

The promyelocytic cell line HL-60 (ATCC #CCL-240) [27] was grown in RPMI-1640 medium supplemented with 10% heat-inactivated fetal bovine serum, L-glutamine (2 mM), streptomycin (100 μg/mL) and penicillin (100 U/mL). The cells were kept at 37 °C, in a humid, 5% CO_2 atmosphere. The cells were sub-cultivated twice a week. The differentiation of these cells to neutrophil-like cells was induced by the addition of DMSO (final concentration of 1.3% v/v) for 4.5 days [28].

2.3. RNA interference assays

Specific sequences of 19 nucleotides of human S100A8 or S100A9 cDNA were selected for the synthesis of small interfering RNAs (siRNA). The pre-annealed siRNAs for S100A8, S100A9, $iPLA_2$ and a non-silencing control were custom-ordered from Eurogentec (Seraing, Belgium). The siRNA sequence for S100A8 was GACCGAGUGUC-CUCAGUAU (forward) and AUACUGAGGACACUCGGUC (reverse) corresponding to the nucleotides 117 to 135. For the S100A9 siRNA

the sequences chosen were AAGAGCUGGUGCGAAAAGA (forward) and UCUUUUCGCACCAGCUCUU (reverse) corresponding to the nucleotides 113 to 131. To knock down $iPLA_2$ a mix of two siRNA was used: CUACGAUGCUCCAGAAACU (forward A), AGUUUCUGGAG-CAUCGUAG (reverse A), GGCGAUCUUGACUCUGCUG (forward B) and CAGCAGAGUCAAGAUCGCC (reverse B). Non-silencing siRNAs had the following sequences AAUUCUCCGAACGUGUCAC (forward) and GUGACACGUUCGGAGAAUU (reverse). Differentiated HL-60 cells were transiently transfected with 1 μg of each siRNA using the Nucleofector apparatus according to the manufacturer's protocol (Amaxa Biosystems, Cologne, Germany). Transfection efficiency was about 80% when using a Nucleofector V kit with program T-019. S100A8/A9 siRNA efficiency has been confirmed previously [10]. Efficiency of $iPLA_2$ siRNA was tested by quantitative real-time PCR, a technique, which will be explained in the next section.

2.4. Quantitative real-time PCR

First-strand cDNA was prepared from 0.5 μg of total RNA, using the Thermoscript™ RT-PCR System and 50 ng/μL of random primers (Invitrogen). Reverse transcription was performed as follows: 10 min at 25 °C, 50 min at 50 °C and 5 min at 85 °C. Two units of RNase H were then added and incubated at 37 °C for 20 min. PCR primers for $iPLA_2$ and actin were designed based on published sequences in GenBank. Real-time PCR was performed on a iQ™5 Real-Time PCR Detection System using iQ™SYBR® Green supermix (Bio-Rad, Herkules, CA, USA) and cDNA synthesized as described above. PCR was performed in a 20 μL reaction volume containing 3 μL of cDNA and 1 μL $iPLA_2$, or actin-specific primer pair. Primer sequences for actin were TGACCCAGAT-CATGTTTGAGA (forward) and AGTCCATCACGATGCCAGT (reverse) and for $iPLA_2$ ATGTCGAAAGACAACGTGGA (forward) and CTCAGCAGAGT-CAAGATCGC (reverse). Cycling conditions consisted of enzyme activation for 3 min at 95 °C followed by denaturation at 95 °C for 15 s and annealing at 60 °C for 30 s (40 cycles). Conditions were optimized to certify similar amplification efficiencies for all products. All experiments were repeated a minimum of three times. Expression level of $iPLA_2$ (Ct) was normalized against the level of mRNA of a housekeeping gene (actin) determined in each sample ($\Delta Ct = Ct_{S100A8/A9} - Ct_{actin}$). ΔCt can be converted into relative RNA expression level ($2^{-\Delta\Delta Ct}$) presuming 100% efficiency for each PCR cycle [29].

2.5. Fluorescence measurements

H_2O_2 production was measured by a fluorescence technique as described in Bueb et al. [30] using a Quantamaster spectrofluorimeter QM-8/2003 (Photon Technology International, Inc., Lawrenceville, NJ, USA). DMSO-differentiated HL-60 cells were loaded with different concentrations of BAPTA-AM or DMSO in PSS containing 0.02% pluronic acid for 30 min at 37 °C, washed three times and resuspended in PSS. 30 μM Amplex Red and 1 U/mL HRP were added during cell incubation, which lasted for 10 min at 37 °C. Cells were then placed in the spectrofluorimeter. Here, H_2O_2 production was measured after stimulation by fMLF (1 μM). The H_2O_2 production of non-silencing siRNA and S100A8/A9 siRNA transfected cells was normalized with respect to their respective controls, which corresponded to the 0 μM BAPTA condition.

2.6. Confocal microscopy

Differentiated HL-60 cells were harvested and washed. 3×10^5 cells were then placed on the coverslips and centrifuged for 5 min at 300 g. After stimulation using different compounds, the cells were fixed in a PBS, which contained 3% w/v paraformaldehyde/2% w/v sucrose, for 15 min at 4 °C. The cells were then washed and permeabilized with a physiological buffer containing 0.1% Triton X-100 and blocked with human IgGs for 15 min. The primary antibody Mac387 (DAKO, Glostrup,

Denmark), directed against an epitope located on S100A9 and detecting also the S100A8/A9 complex, was applied to the cells at 1:200 dilution for 45 min at room temperature. A mouse serum (Jackson Immuno Research, Newmarket Suffolk, UK) was used as a negative control in order to observe unspecific labeling of the detection system. The cells were washed three times and then incubated with a cyanin™2-conjugated donkey anti-mouse secondary antibody (Jackson Immuno Research). The coverslips were washed four times, mounted in Moviol/DABCO and stored for 12 h at 4 °C in the dark. Fluorescence images were acquired using the laser-scanning confocal microscope LSM510 (Carl Zeiss, Zaventem, Belgium) with a 488 nm laser and a band pass BP505–550 nm to respectively excite and detect cyanin™2.

2.7. Confocal microscopy quantification

All confocal microscopy images were taken with a LSM 510 confocal microscope where the pinhole was adjusted to 1 Airy unit and using a Plan-Apochromat 63×/1.40 DIC oil objective (Carl Zeiss). A minimum of 100 cells in total were counted per condition. Imaged dHL-60 cells, stimulated (test) with different agonists (fMLF, thapsigargin, PMA) under different calcium conditions ($\pm$extracellular Ca^{2+} or $\pm$BAPTA-AM), were quantified in terms of cells displaying a positive (S100 pos) or negative (S100 neg) S100A8/A9 plasma membrane translocation. Results are normalized with respect to their control (ctrl) using the following formula:

$$Fold\,induction = \frac{S100\,pos_{(test)}}{\left[S100\,pos_{(test)} + S100\,neg_{(test)}\right]} \Big/ \frac{S100\,pos_{(ctrl)}}{\left[S100\,pos_{(ctrl)} + S100\,neg_{(ctrl)}\right]}.$$

With respect to the dHL-60 cells treated with kinase or phospholipase inhibitors (inhib) or without inhibitors (ctrl), images of dHL-60 displaying a positive S100A8/A9 plasma membrane translocation were counted and normalized to cells stimulated with (w fMLF) or without (w/o fMLF) fMLF by using the following formula:

$$\%\,Translocation = \frac{HL\text{-}60_{(inhib)\,(w\,fMLF)} - HL\text{-}60_{(inhib)\,(w/o\,fMLF)}}{HL\text{-}60_{(ctrl)\,(w\,fMLF)} - HL\text{-}60_{(ctrl)\,(w/o\,fMLF)}} \times 100.$$

2.8. p38 MAPK assay

The p38 MAPK activity was measured by using the p38 MAPK activity kit according to the manufacturer's protocol (Cell Signaling Technology, Danvers, MA, USA). Briefly, cells were pre-treated for 30 min at 37 °C with kinase or phospholipase inhibitors and then stimulated for 1 min with fMLF. After cell lysis, phosphorylated p38 MAPK was immunoprecipitated with a phospho p38 MAPK antibody from 200 μg of lysate. The immune complex was washed and resuspended in a kinase buffer containing 200 μM ATP and 1 μg of recombinant activating factor-2 (ATF-2) as a p38 MAPK substrate. The reaction was carried out at 30 °C for 30 min and terminated by adding an SDS sample buffer. The kinase reaction was analyzed by Western blotting with a phospho-specific ATF-2 antibody.

2.9. Metabolic labeling

Phosphorylation of S100A9 was investigated by metabolic labeling of differentiated HL-60 cells with inorganic [^{32}P]-phosphate (Hartman Analytics, Braunschweig, Germany). 10×10^6 cells were incubated in a phosphate-free buffer (HEPES 20 mM, glucose 5.5 mM, CaCl$_2$ 1.8 mM, KCl 5.4 mM, NaCl 137 mM, 1% (w/v) BSA, pH 7.2) for 1 h. Thereafter, the cells were incubated with 40 μCi [^{32}P]-phosphate. After 60 min of incubation, the inhibitors were added for 30 min. Then the cells were stimulated by fMLF. Phosphate incorporation into proteins was detected by phosphorimaging of the dried gel (GE Healthcare,

Buckinghamshire, UK) after immunoprecipitation of S100A9 (with Mac387 antibody) and sample migration by SDS-PAGE (16% Tricine pre-cast gel from Invitrogen). Equal loading of immunoprecipitated S100A9 was confirmed by Western blotting using affinity purified rabbit antisera monospecific for S100A9 (kindly provided by Dr T. Vogl).

2.10. iPLA$_2$ assay

iPLA$_2$ activity was measured using a kit from Cayman Chemicals following the manufacturer's instructions (Cayman Chemicals, Ann Arbor, MI, USA). After appropriate treatment and centrifugation of the cells, the pellets were resuspended in 1 mL of cold buffer (50 M Hepes, pH 7.4, containing 1 mM EDTA) and sonicated. Cell lysates were centrifuged at 10 000 rpm for 15 min at 4 °C. 10 μl of the lysate were added to a 96 well microtiter plate followed by 5 μL of assay buffer (80 mM Hepes pH 7.4, 150 mM NaCl, 4 mM Triton X-100, 30% glycerol, and 1 mg/mL BSA). The reaction was initiated by the addition of 200 μl of arachidonoyl thiophosphatidylcholin dissolved in 2× assay buffer and incubated at room temperature for 60 min. The reaction was terminated by adding 10 μl of 25 mM 5,5-dithio-bis(2-nitrobenzoic acid), 475 mM EGTA in 0.5 M Tris–HCl pH 8.0. The absorbance was measured at 414 nm in a sunrise microtiter plate reader (TECAN, Mechelen, Belgium). iPLA$_2$ activity was first normalized with respect to the protein content of each sample and then expressed as the fold induction as compared to non-stimulated control.

2.11. Statistics

Values obtained from the different cell batches were expressed as the mean $\pm$ standard error of the mean (SEM), where $n \geq 3$. Statistical analysis was performed using the Prism5 software (Graph Pad Software, La Jolla, CA, USA). An analysis of the variance, ANOVA, was followed by the Newman–Keuls pairwise comparison test for multiple sets of data or by the Student's t-test for the comparison of only two sets of data. Values of $p < 0.05$ indicate that the difference between the means should be considered statistically significant. In the figures presented in the following section, asterisks indicate the level of significance: $* = p < 0.05$; $** = p < 0.01$; $*** = p < 0.001$.

3. Results

3.1. Relationship between S100A8/A9 complex, $[Ca^{2+}]_i$ elevation and NOX2 activation in differentiated HL-60 cells

We investigated S100A8/A9 as a possible link between Ca^{2+} elevation and H$_2$O$_2$ production in neutrophil-like DMSO-differentiated HL-60 cells by measuring H$_2$O$_2$ production in scrambled or S100A8/A9 siRNA transfected cells in different $[Ca^{2+}]_i$ conditions by using increasing concentrations of the $[Ca^{2+}]_i$ chelator BAPTA. H$_2$O$_2$ production of non-silencing siRNA and S100A8/A9 siRNA transfected cells (Fig. 1A) were expressed as % of their respective controls (0 μM BAPTA). In control siRNA transfected cells our results indicate that by increasing BAPTA concentrations up to 3 μM, H$_2$O$_2$ production is fully inhibited, suggesting the Ca^{2+}-dependence of H$_2$O$_2$ production (Fig. 1A). Moreover the transfection of S100A8/A9 siRNA incubated without BAPTA leads to a 40% inhibition of H$_2$O$_2$ production (Fig. 1 insert), when compared to the control siRNA transfected cells, confirming the importance of S100A8/A9 for NOX2 activation in dHL-60 cells. In the S100A8/A9 siRNA transfected cells, the BAPTA curve shows that H$_2$O$_2$ production is inhibited at low BAPTA concentrations (0.01 μM–0.3 μM), indicating a link between S100A8/A9 and $[Ca^{2+}]_i$ for NOX2 activation.
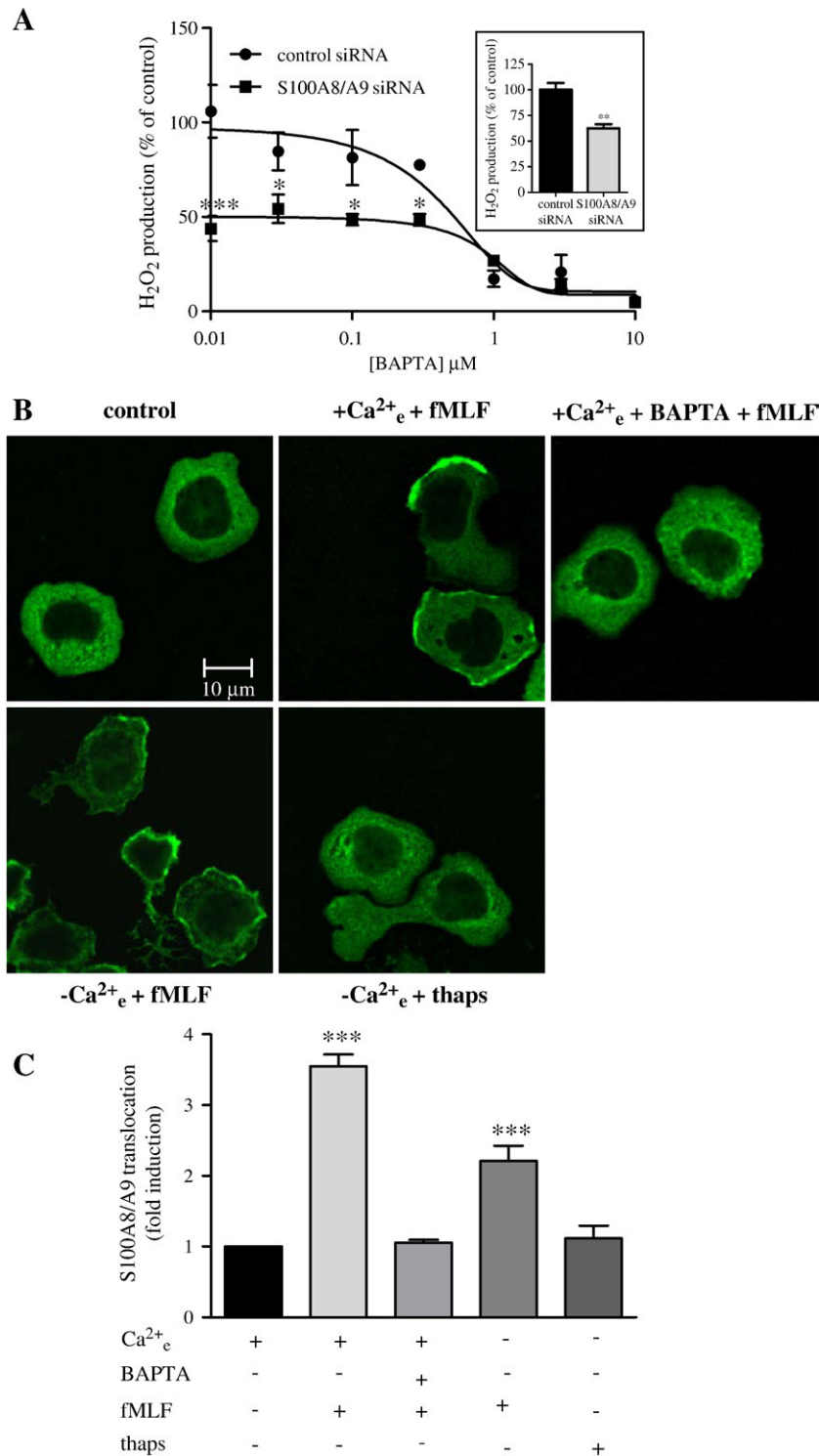
Fig. 1. Ca^{2+} dependence of S100A8/A9 translocation and S100A8/A9 dependence of NOX2 activity. A) Measurement of H_2O_2 production. Differentiated HL-60 (dHL-60) cells were transiently transfected with S100A8 and S100A9 or non-silencing siRNA (control siRNA). After 48 h, cells were tested for fMLF (1 μM)-induced H_2O_2 production in the presence of increasing concentrations of BAPTA (0.01–10 μM). H_2O_2 production is expressed as a percentage (%) of the control (0 μM BAPTA). The results are expressed as mean ± SEM. Asterisks (*/**/***) indicate that the sample is significantly different from control with the following levels of statistical significance: * = $p<0.05$; *** = $p<0.01$; *** = $p<0.001$. Insert: H_2O_2 production was measured 48 h after S100A8/A9 or control siRNA transfection and represented as % of control (control siRNA transfected cells). Results are expressed as mean ± SEM and two asterisks, **, indicate that the sample is significantly different from the control. B) Immunofluorescent labeling of S100A8/A9. dHL-60 cells were incubated in the presence (upper panels) or absence (lower panels) of extracellular Ca^{2+} (1.25 mM) or with BAPTA (3 μM) (upper right panel). Then, cells were stimulated with fMLF (1 μM) (upper middle, right panel and lower left panel), thapsigargin (0.1 μM) (lower right panel) or DMSO as control (upper left panel). S100A8/A9 were stained by the monoclonal antibody Mac387 followed by a cyanin™2-labeled secondary antibody. C) Quantification of S100A8/A9 translocation was determined as described in Section 2, Materials and methods. In this graph, the asterisks, ***, indicate that the sample is significantly different from control (DMSO-treated cells) with a probability less than 0.001 ($p<0.001$).

A

genistein	-	-	+	-
SB203580	-	-	-	+
fMLF	-	+	+	+

B

genistein	-	-	+	-
SB203580	-	-	-	+
fMLF	-	+	+	+

C

genistein	-	-	+	-
SB203580	-	-	-	+
fMLF	-	+	+	+

D

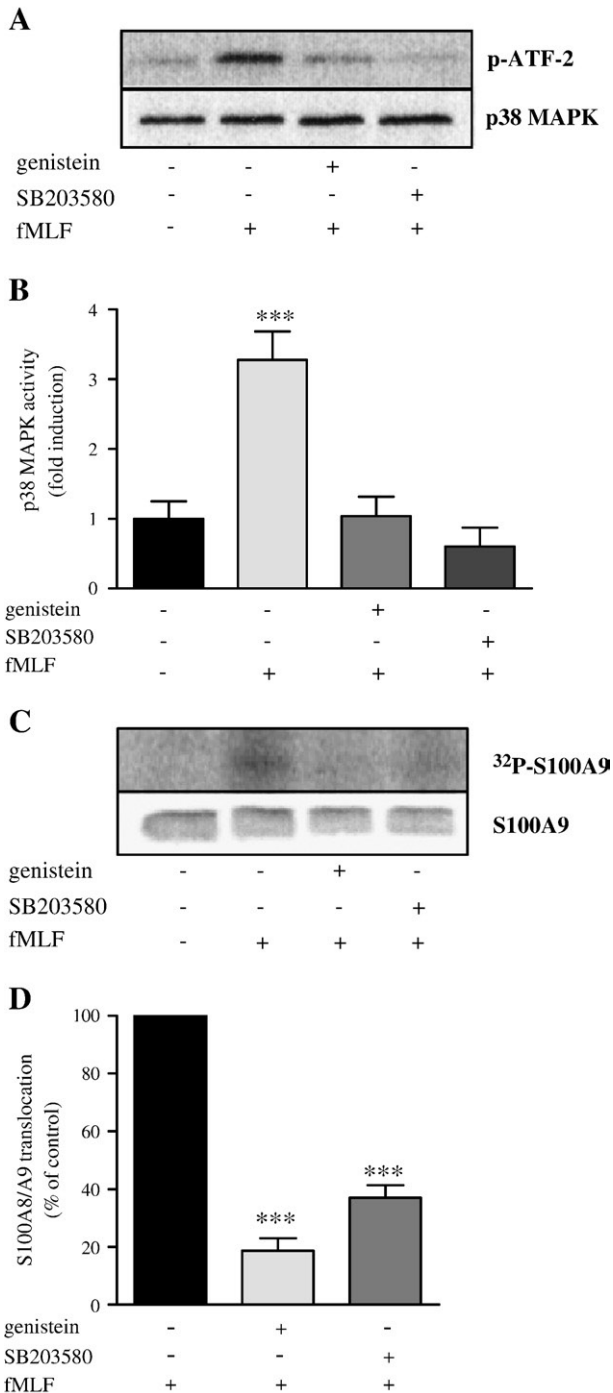|			
genistein	-	+	-
SB203580	-	-	+
fMLF	+	+	+

Fig. 2. S100A8/A9 translocation is dependent on p38 MAPK-mediated S100A9 phosphorylation. p38 MAPK activity was measured by using the p38 MAPK activity kit from Cell Signaling Technology (as described in Section 2, Materials and methods). A) dHL-60 cells were stimulated with fMLF (1 μM) or DMSO as control after pretreatment for 30 min with either genistein (100 μM) or SB203580 (10 μM). The immunoprecipitated p38 MAPK was resuspended in kinase buffer containing ATP and recombinant ATF-2. Phospho-ATF-2 was detected by Western blotting using an anti-phospho-ATF-2 antibody and the input of the reaction was determined by measuring total p38 MAPK. B) The amount of phospho-ATF-2 was normalized with respect to the input of total p38 MAPK and compared to the control (DMSO-treated cells). C) S100A9 phosphorylation was investigated by metabolic labeling of cells with inorganic [^{32}P]-phosphate. Cells were stimulated with fMLF (1 μM) or DMSO as control in the presence of either genistein (100 μM) or SB203580 (10 μM). Equal loading of immunoprecipitated S100A9 was tested by Western blotting using affinity purified rabbit antisera monospecific for S100A9. Graph D corresponds to the quantification of the S100A8/A9 translocation determined as described in Section 2, Materials and methods. Three asterisks, ***, indicate that the sample is significantly different from the control (fMLF-stimulated cells), with a probability less than 0.001 ($p < 0.001$).

3.2. Intracellular Ca^{2+} store depletion is required for S100A8/A9 translocation

Previous studies [20,21] have indicated that S100 translocation is dependent on Ca^{2+}. Moreover, since our data established that NOX2 activation acquired Ca^{2+} sensitivity via S100A8/A9, it is possible that the S100A8/A9 complex, through its Ca^{2+}-dependent translocation to the plasma membrane, may act as a 'molecular switch' between $[Ca^{2+}]_i$ elevation and NOX2 activation. To test this hypothesis, we incubated dHL-60 cells with or without BAPTA and monitored the endogenous S100A8/A9 translocation by confocal immunofluorescence. In the non-stimulated cells, S100A8/A9 is homogeneously distributed within the cytosol (Fig. 1B control). fMLF (1 μM) stimulation resulted in a 3.5 fold increased recruitment of S100A8/A9 to the plasma membrane (Fig. 1B upper middle panel and 1C). Incubation with BAPTA (3 μM, corresponding to the maximal inhibition of H_2O_2 production) prevented the fMLF-stimulated S100A8/A9 redistribution (Fig. 1B upper right panel and 1C). We conclude that $[Ca^{2+}]_i$ elevations are thus necessary for S100A8/A9 relocalization at the plasma membrane.

In neutrophils, $[Ca^{2+}]_i$ elevation results from an intracellular or extracellular Ca^{2+} mobilization either through the internal store depletion or Ca^{2+} influx [31]. To identify Ca^{2+} pools implicated in S100A8/A9 translocation, we stimulated dHL-60 cells with fMLF (1 μM) in the absence of extracellular Ca^{2+}. In these conditions, although S100A8/A9 translocation is partially decreased, a significant membrane recruitment of the S100A8/A9 complex is still observed (Fig. 1B lower left panel and 1C), providing evidence that intracellular Ca^{2+} store depletion can be sufficient for a membrane redistribution of S100 complex. On the other hand, a passive Ca^{2+} release from the internal stores by thapsigargin [32] in extracellular Ca^{2+}-free conditions was not able to induce S100A8/A9 membrane recruitment (Fig. 1B lower right panel and 1C). The same result was obtained when cells were stimulated by thapsigargin in presence of 1.25 μM of Ca^{2+} (data not shown). Taken together, these results indicate that $[Ca^{2+}]_i$ elevation via store depletion is necessary, but probably not sufficient, for S100A8/A9 complex membrane recruitment.

3.3. S100A9 phosphorylation by p38 MAPK is involved in the S100A8/A9 translocation

Given that Ca^{2+} release from the stores is necessary but not sufficient for S100 complex translocation, we assume that an additional signal is required for S100A8/A9 redistribution. Since it has been established that S100A9 can be phosphorylated on Thr 113 by p38 MAPK [23,24], we questioned whether the phosphorylation of S100A9 by p38 MAPK is involved in S100A8/A9 translocation. To test this hypothesis, we used a pharmacological approach to study the S100A8/A9 translocation after treatment with the tyrosine kinase inhibitor genistein or the p38 MAPK inhibitor SB203580. Decrease of S100A9 phosphorylation by genistein (100 μM) was accompanied by inhibition of S100A8/A9 translocation (80 ± 4%) (Fig. 2C and D), confirming the correlation between S100A9 phosphorylation and S100A8/A9 translocation. Furthermore, p38 MAPK activity inhibition by SB203580 (10 μM) (Fig. 2A and B) also resulted in a decrease of S100A9 phosphorylation, which was associated with a reduction of S100A8/A9 membrane recruitment (60 ± 4%). We can conclude that in addition to the internal Ca^{2+} store release, p38 MAPK-mediated phosphorylation of S100A9 is involved in S100A8/A9 complex redistribution to the plasma membrane.

3.4. $iPLA_2$ is a novel mediator of S100A8/A9 translocation and NOX2 activity

Our results establish that S100A8/A9 complex modulates NOX2 activity through p38 MAPK-dependent and intracellular Ca^{2+} store depletion-dependent translocation of the S100 complex. In a previous study, Beckett et al. suggested that p38 MAPK activation occurs downstream of $iPLA_2$ activation [26] in myocytes. Therefore, we suppose that $iPLA_2$-mediated p38 MAPK activation is involved in
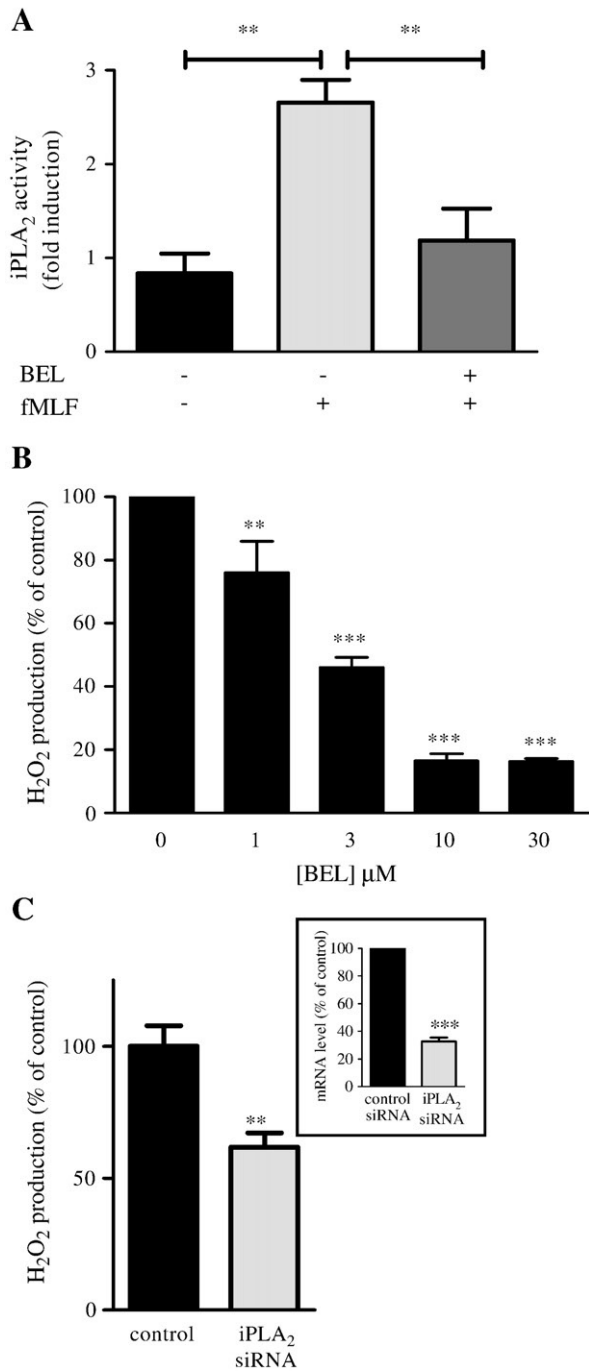
Fig. 3. NOX2 activity is dependent on iPLA$_2$. A) iPLA$_2$ activity was measured by using the iPLA$_2$ assay kit from Cayman chemicals (as described in Section 2, Materials and methods). dHL-60 cells were stimulated with fMLF (1 μM) or DMSO as control in the absence or presence of BEL (10 μM). Results were normalized with respect to the control (DMSO-treated cells) and expressed as mean ± SEM. In all the graphs of this figure, two asterisks, **, indicate that the sample is significantly different from the control with a probability less than 0.01 ($p<0.01$) and three asterisks ***, indicate that the sample is significantly different from the control with a probability less than 0.001 ($p<0.001$). B) H$_2$O$_2$ production was measured by a spectrofluorimetric method after incubation for 30 min with increasing concentrations of BEL (1–30 μM). Results are expressed as % of control (0 μM BEL). C) dHL-60 cells were transiently transfected with iPLA$_2$ or non-silencing siRNA (control). After 48 h, cells were tested for fMLF (1 μM)-induced H$_2$O$_2$ production. Results are expressed as % of control. Efficiency of iPLA$_2$ siRNA tested by quantitative real-time PCR is shown in insert. Data were normalized to actin and expressed relative to the control (non-silencing siRNA). Results are expressed as mean ± SEM.

S100A8/A9 translocation-regulated NOX2 activity in dHL-60 cells. To test this hypothesis, we first determined whether iPLA$_2$ is activated in dHL-60 cells and then investigated its potential involvement in NOX2
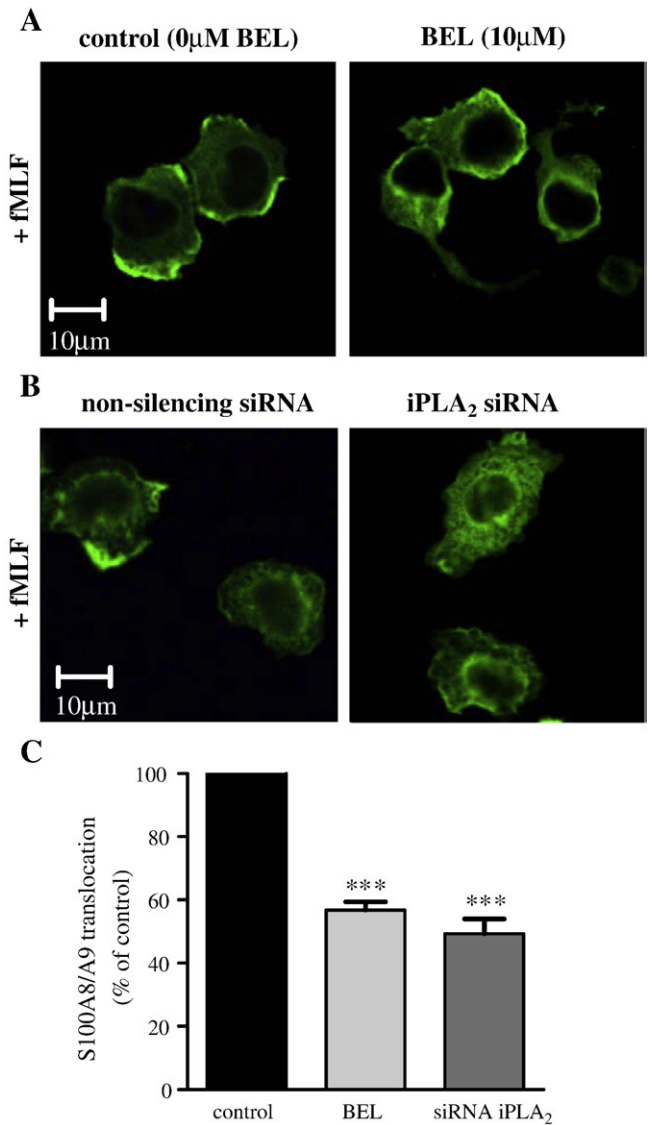

Fig. 4. S100A8/A9 translocation is dependent on iPLA$_2$. Immunofluorescent labeling of S100A8/A9. A) dHL-60 cells were stimulated with fMLF (1 μM) after pretreatment of the cells with BEL (10 μM) or without BEL (control). B) Cells were transiently transfected with iPLA$_2$ or non-silencing siRNA (control). After 48 h, cells were stimulated with fMLF (1 μM) or DMSO as control. C) Quantification of S100A8/A9 translocation as described in Section 2, Materials and methods. Three asterisks ***, indicate that the sample is significantly different from the control with a probability less than 0.001 ($p<0.001$).

activation. Measurement of iPLA$_2$ activity demonstrated that fMLF-stimulated dHL-60 cells led to a 2.7 fold increase in iPLA$_2$ activity (Fig. 3A). Pretreatment of cells with 10 μM bromoenol lactone (BEL), a selective inhibitor of iPLA$_2$ [33], resulted in a complete inhibition of fMLF-induced iPLA$_2$ activity (Fig. 3A). These results confirm that iPLA$_2$ is functionally active in dHL-60 cells.

Two independent approaches (pharmacological and siRNA strategy) were used to determine the role of iPLA$_2$ in NOX2 regulation. Pretreatment of dHL-60 cells with BEL (10 μM) triggered a concentration-dependent inhibition of fMLF-induced H$_2$O$_2$ production (83 ±2% inhibition, 10 μM BEL) (Fig. 3B). To confirm this result, dHL-60 cells were transfected with specific iPLA$_2$ siRNA. As expected, siRNA decreased iPLA$_2$ RNA expression by 70% when compared to the non-silencing siRNA transfected control cells (Fig 3C insert). Further, iPLA$_2$ siRNA prevented activation of fMLF-induced NOX2 activation (Fig. 3C). Similar effects of the siRNA strategy and pharmacological inhibition of iPLA$_2$-regulated NOX2 activity underline the role of iPLA$_2$ in this process in dHL-60 cells. These two approaches were also used to determine
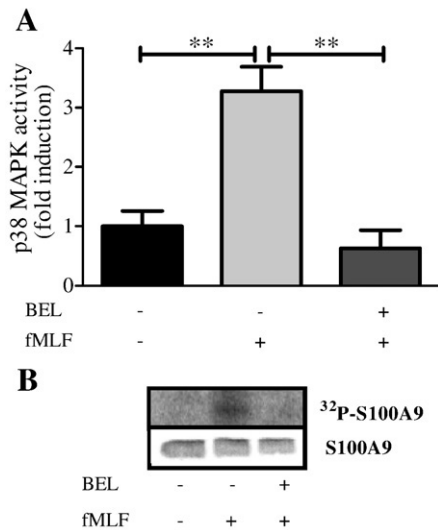
A

B

Fig. 5. iPLA$_2$ is implicated in the activation of p38 MAPK and phosphorylation of S100A9. A) Measurement of p38 MAPK activity. dHL-60 cells were stimulated with fMLF (1 μM) or DMSO as control after treatment of the cells with or without BEL (10 μM). The phospho-ATF-2 amount was normalized to the input of total p38 MAPK and compared to the control (DMSO-treated cells). Two asterisks, **, indicate that the sample is significantly different from the non-stimulated control with a probability less than 0.01 (p<0.01). B) S100A9 phosphorylation determined by metabolic labeling. Cells were stimulated with fMLF (1 μM) or DMSO as control after 30 min incubation with or without BEL (10 μM). Equal loading of immunoprecipitated S100A9 was tested by Western blotting using affinity purified rabbit antisera monospecific for S100A9.

whether iPLA$_2$ regulated NOX2 activity through S100A8/A9 transloca-tion. As shown in Fig. 4A, fMLF-stimulated S100A8/A9 recruitment to the plasma membrane was inhibited (44±2%) by pretreatment of the cells with BEL (10 μM). Similarly, S100A8/A9 translocation was reduced (51±4%) after transfection of cells by iPLA$_2$ siRNA (Fig. 4B). Our results indicate that fMLF-mediated activation of NOX2 is dependent on iPLA$_2$ activation-mediated S100A8/A9 translocation in dHL-60 cells.

To test whether iPLA$_2$ activity is necessary for p38 MAPK activation, we pre-treated dHL-60 cells with BEL (10 μM) before fMLF (1 μM) stimulation and measured p38 MAPK activity. As shown in Fig. 5A, fMLF-activated p38 MAPK is prevented by pretreatment with BEL. Thus, iPLA$_2$ appears to regulate fMLF-stimulated p38 MAPK activity in dHL-60 cells. Besides, ^{32}P metabolic labeling showed a decrease of fMLF-stimulated S100A9 phosphorylation (Fig. 5B) after BEL pretreatment. These results demonstrate that S100A8/A9 translocation mediated by p38 MAPK-induced S100A9 phosphorylation is dependent on iPLA$_2$ and that activation of p38 MAPK occurs downstream of iPLA.

4. Discussion

S100A8 and S100A9, which are found in high concentrations at local sites of inflammation, are also largely expressed in the cytoplasm of phagocytes [6,11,34]. These two Ca^{2+}-binding proteins have been involved in the regulation of NOX2 in a Ca^{2+}-dependent manner [7,8]. Studies regarding the regulation of NOX2 by S100 proteins have largely been performed in cell-free assays or recombinant systems. Thus conclusions might be carefully extrapolated to whole cells and even to human neutrophils. However, the exact regulatory mechanism involving Ca^{2+}, S100A8/A9 and NOX2 activity is not completely clear. Therefore fundamental details, in particular the contribution of S100A8/A9 in the Ca^{2+}-regulated NOX2 activity as well as in the pathway underlying S100-regulated NOX2 activity, need to be understood. Our present work investigated the role of S100 A8/A9 in the regulation of NOX2 activity in neutrophil-like HL-60 cells. We found that both S100A8/A9 complex and [Ca^{2+}]$_i$ elevation are essential for NOX2 activation in these cells [10].

The molecular mechanism by which S100A8/A9 facilitates the [Ca^{2+}]$_i$ elevation-dependent NOX2 activity is unclear. Previously, it has been

shown that S100A8/A9, through its binding to Ca^{2+}, interacts with flavocytochrome b_{558} and mediates its transition from an inactive to an active conformation state resulting in NOX2 activation [35]. These results raise the question as to how cytosolic S100A8/A9 localizes towards the plasma membrane where it combines to NOX2. Clearly, there is evidence that the S100A8/A9 complex migrates to the membrane through a Ca^{2+}-dependent mechanism [20–22] but the Ca^{2+} source leading to Ca^{2+} mobilization has not yet been formally identified. Our results, based on an immunofluorescence approach, confirm the importance of [Ca^{2+}]$_i$ elevation in S100A8/A9 membrane recruitment and indicate that Ca^{2+} released from the internal stores is necessary for fMLF-induced S100A8/A9 translocation to the plasma membrane in differentiated HL-60 cells. In addition, a partial reduction of S100A8/A9 translocation is observed after extracellular Ca^{2+} deprivation. Thus, we can conclude that although extracellular Ca^{2+} entry is not crucial for S100A8/A9 translocation, it appears that it is required for a maximal translocation, in addition to the Ca^{2+} emptying from the intracellular stores. Stimulation of cells with thapsigargin, in the absence of extra-cellular Ca^{2+} did not induce the redistribution of S100A8/A9 to the plasma membrane. While fMLF induces a fast receptor-mediated Ca^{2+} store depletion ensuring a rapid increase in [Ca^{2+}]$_i$, thapsigargin trig-gers a passive Ca^{2+} release from the internal stores and a slow increase in [Ca^{2+}]$_i$ [36,37]. The discrepancy between these two Ca^{2+} kinetic processes may explain why the S100A8/A9 complex translocates upon fMLF and not thapsigargin stimulation. However, we cannot exclude the possibility that a supplementary signal is necessary for S100A8/A9 translocation to the plasma membrane. This is supported by the fact that p38 MAPK-mediated S100A9 phosphorylation [23,24] has been involved in the membrane recruitment of S100A8/A9 in cellular fractionation experiments [38,39]. In dHL-60 cells, our data demonstrate that S100A9 phosphorylation and S100A8/A9 translocation are inhib-ited after treatment of cells with tyrosin kinase and p38 MAPK inhi-bitors. This result supports the idea that p38 MAPK-induced S100A9 phosphorylation is necessary for S100A8/A9 relocalization. It could be envisaged that phosphorylation increases S100A9 affinity for Ca^{2+} and therefore favors Ca^{2+} binding to S100A9 [39] leading to improved S100A8/A9 translocation to the plasma membrane.

In myocytes there is evidence for p38 MAPK activation by iPLA$_2$ [26], but there is no indication of iPLA$_2$ involvement in S100A9 phosphorylation. We have shown that iPLA$_2$ is required for S100A9 phosphorylation and activation of p38 MAPK is induced by iPLA$_2$ in dHL-60 cells. Because iPLA$_2$ induces S100A9 phosphorylation through p38 MAPK, it would be expected that iPLA$_2$ regulates S100A8/A9 translocation and subsequent NOX2 activity. Our data based on the use of a pharmacological inhibitor and a siRNA strategy support the hypothesis that iPLA$_2$ controls S100 complex translocation and NOX2 activity. Thus we identify iPLA$_2$ as a new molecular player in S100A8/A9 translocation-mediated NOX2 activity. Because PLA$_2$-produced arachidonic acid has been shown to regulate NOX2 activity [8], most likely through the process of binding to S100A8/A9 which allows its transport to the plasma membrane [40], we cannot fully exclude the possibility that iPLA$_2$ mediates an additional mechanism involved in the regulation of NOX2 activity and/or S100A8/A9 translocation, independently of p38 MAPK activity. However, intracellular Ca^{2+} store depletion, which is involved in S100A8/A9 translocation in dHL-60 cells, has been suggested to activate iPLA$_2$ [41] through the production of a diffusible messenger [42]. This mediator has been identified as sphingosine-1 phosphate by Itagaki et al. [43] in human neutrophils. Further investigations will be necessary to determine the actual relationship between sphingosine-1 phosphate/iPLA$_2$/p38 MAPK leading to S100A8/A9 translocation and NOX2 activation.

In conclusion, we establish that fMLF-induced NOX2 activation occurs via S100A8/A9 complex translocation to the plasma membrane resulting from (i) S100A9 phosphorylation and (ii) an increase of [Ca^{2+}]$_i$ induced by intracellular Ca^{2+} store depletion. Most importantly, our results here allow us to define a signal transduction pathway linking

iPLA$_2$-regulated p38 MAPK activity to S100A8/A9 translocation and subsequent NOX2 activation.

Acknowledgements

References

[1] B.M. Babior, Oxidants from phagocytes: agents of defense and destruction, Blood 64 (1984) 959–966.

[2] B.M. Babior, Phagocytes and oxidative stress, Am. J. Med. 109 (2000) 33–44.

[3] F. Valentin, J. Bueb, C. Capdeville-Atkinson, E. Tschirhart, Rac-1-mediated O$_2^-$ secretion requires Ca^{2+} influx in neutrophil-like HL-60 cells, Cell Calcium 29 (2001) 409–415.

[4] S. Bréchard, J.L. Bueb, E.J. Tschirhart, Interleukin-8 primes oxidative burst in neutrophil-like HL-60 through changes in cytosolic calcium, Cell Calcium 37 (2005) 531–540.

[5] J.W. Putney Jr., A model for receptor-regulated calcium entry, Cell Calcium 7 (1986) 1–12.

[6] P.A. Hessian, J. Edgeworth, N. Hogg, MRP-8 and MRP-14, two abundant Ca(2+)-binding proteins of neutrophils and monocytes, J. Leukoc. Biol. 53 (1993) 197–204.

[7] J. Doussière, F. Bouzidi, P.V. Vignais, The S100A8/A9 protein as a partner for the cytosolic factors of NADPH oxidase activation in neutrophils, Eur. J. Biochem. 269 (2002) 3246–3255.

[8] S. Berthier, M.H. Paclet, S. Lerouge, F. Roux, S. Vergnaud, A.W. Coleman, F. Morel, Changing the conformation state of cytochrome b558 initiates NADPH oxidase activation: MRP8/MRP14 regulation, J. Biol. Chem. 278 (2003) 25499–25508.

[9] C. Kerkhoff, W. Nacken, M. Benedyk, M.C. Dagher, C. Sopalla, J. Doussiere, The arachidonic acid-binding protein S100A8/A9 promotes NADPH oxidase activation by interaction with p67phox and Rac-2, FASEB J. 19 (2005) 467–469.

[10] V. Schenten, S. Bréchard, C. Melchior, S. Plançon, A. Salsmann, E.J. Tschirhart, Ca^{2+}-dependent regulation of NOX2 activity via MRP proteins in HL-60 granulocytes, Calcium Binding Proteins 3 (2008) 25–27.

[11] J. Edgeworth, M. Gorman, R. Bennett, P. Freemont, N. Hogg, Identification of p8, 14 as a highly abundant heterodimeric calcium binding protein complex of myeloid cells, J. Biol. Chem. 266 (1991) 7706–7713.

[12] N. Leukert, C. Sorg, J. Roth, Molecular basis of the complex formation between the two calcium-binding proteins S100A8 (MRP8) and S100A9 (MRP14), Biol. Chem. 386 (2005) 429–434.

[13] T. Vogl, J. Roth, C. Sorg, F. Hillenkamp, K. Strupat, Calcium-induced noncovalently linked tetramers of MRP8 and MRP14 detected by ultraviolet matrix-assisted laser desorption/ionization mass spectrometry, J. Am. Soc. Mass Spectrom. 10 (1999) 1124–1130.

[14] N. Leukert, T. Vogl, K. Strupat, R. Reichelt, C. Sorg, J. Roth, Calcium-dependent tetramer formation of S100A8 and S100A9 is essential for biological activity, J. Mol. Biol. 359 (2006) 961–972.

[15] A. Rammes, J. Roth, M. Goebeler, M. Klempt, M. Hartmann, C. Sorg, Myeloid-related protein (MRP) 8 and MRP14, calcium-binding proteins of the S100 family, are secreted by activated monocytes via a novel, tubulin-dependent pathway, J. Biol. Chem. 272 (1997) 9496–9502.

[16] N. Anceriz, K. Vandal, P.A. Tessier, S100A9 mediates neutrophil adhesion to fibronectin through activation of beta2 integrins, Biochem. Biophys. Res. Commun. 354 (2007) 84–89.

[17] C. Ryckman, S.R. McColl, K. Vandal, R. de Medicis, A. Lussier, P.E. Poubelle, P.A. Tessier, Role of S100A8 and S100A9 in neutrophil recruitment in response to monosodium urate monohydrate crystals in the air-pouch model of acute gouty arthritis, Arthritis Rheum. 48 (2003) 2310–2320.

[18] B.W. Schafer, C.W. Heizmann, The S100 family of EF-hand calcium-binding proteins: functions and pathology, Trends Biochem. Sci. 21 (1996) 134–140.

[19] J. Roth, S. Teigelkamp, M. Wilke, L. Grun, B. Tummler, C. Sorg, Complex pattern of the myelo-monocytic differentiation antigens MRP8 and MRP14 during chronic airway inflammation, Immunobiology 186 (1992) 304–314.

[20] R.S. Bhardwaj, C. Zotz, G. Zwadlo-Klarwasser, J. Roth, M. Goebeler, K. Mahnke, M. Falk, G. Meinardus-Hager, C. Sorg, The calcium-binding proteins MRP8 and MRP14 form a membrane-associated heterodimer in a subset of monocytes/macrophages present in acute but absent in chronic inflammatory lesions, Eur. J. Immunol. 22 (1992) 1891–1897.

[21] P. Lemarchand, M. Vaglio, J. Mauel, M. Markert, Translocation of a small cytosolic calcium-binding protein (MRP-8) to plasma membrane correlates with human neutrophil activation, J. Biol. Chem. 267 (1992) 19379–19382.

[22] J. Roth, F. Burwinkel, C. van den Bos, M. Goebeler, E. Vollmer, C. Sorg, MRP8 and MRP14, S-100-like proteins associated with myeloid differentiation, are translocated to plasma membrane and intermediate filaments in a calcium-dependent manner, Blood 82 (1993) 1875–1883.

[23] G. Lominadze, M.J. Rane, M. Merchant, J. Cai, R.A. Ward, K.R. McLeish, Myeloid-related protein-14 is a p38 MAPK substrate in human neutrophils, J. Immunol. 174 (2005) 7257–7267.

[24] T. Vogl, S. Ludwig, M. Goebeler, A. Strey, I.S. Thorey, R. Reichelt, D. Foell, V. Gerke, M.P. Manitz, W. Nacken, S. Werner, C. Sorg, J. Roth, MRP8 and MRP14 control microtubule reorganization during transendothelial migration of phagocytes, Blood 104 (2004) 4260–4268.

[25] M.J. Rane, S.L. Carrithers, J.M. Arthur, J.B. Klein, K.R. McLeish, Formyl peptide receptors are coupled to multiple mitogen-activated protein kinase cascades by distinct signal transduction pathways: role in activation of reduced nicotinamide adenine dinucleotide oxidase, J. Immunol. 159 (1997) 5070–5078.

[26] C.S. Beckett, K. Pennington, J. McHowat, Activation of MAPKs in thrombin-stimulated ventricular myocytes is dependent on Ca^{2+}-independent PLA$_2$, Am. J. Physiol. Cell Physiol. 290 (2006) C1350–C1354.

[27] S.J. Collins, R.C. Gallo, R.E. Gallagher, Continuous growth and differentiation of human myeloid leukaemic cells in suspension culture, Nature 270 (1977) 347–349.

[28] P. Harris, P. Ralph, Human leukemic models of myelomonocytic development: a review of the HL-60 and U937 cell lines, J. Leukoc. Biol. 37 (1985) 407–422.

[29] K.J. Livak, T.D. Schmittgen, Analysis of relative gene expression data using real-time quantitative PCR and the 2(− Delta Delta C(T)) Method, Methods 25 (2001) 402–408.

[30] J.L. Bueb, A. Gallois, J.C. Schneider, J.P. Parini, E. Tschirhart, A double-labelling fluorescent assay for concomitant measurements of [Ca^{2+}]$_i$ and O$_2^-$ production in human macrophages, Biochim. Biophys. Acta 1244 (1995) 79–84.

[31] J.W. Putney Jr., Pharmacology of capacitative calcium entry, Mol. Interv. 1 (2001) 84–94.

[32] O. Thastrup, P.J. Cullen, B.K. Drobak, M.R. Hanley, A.P. Dawson, Thapsigargin, a tumor promoter, discharges intracellular Ca^{2+} stores by specific inhibition of the endoplasmic reticulum Ca(2+)-ATPase, Proc. Natl. Acad. Sci. U. S. A. 87 (1990) 2466–2470.

[33] J. Balsinde, I.D. Bianco, E.J. Ackermann, K. Conde-Frieboes, E.A. Dennis, Inhibition of calcium-independent phospholipase A2 prevents arachidonic acid incorporation and phospholipid remodeling in P388D1 macrophages, Proc. Natl. Acad. Sci. U. S. A. 92 (1995) 8527–8531.

[34] K. Odink, N. Cerletti, J. Bruggen, R.G. Clerc, L. Tarcsay, G. Zwadlo, G. Gerhards, R. Schlegel, C. Sorg, Two calcium-binding proteins in infiltrate macrophages of rheumatoid arthritis, Nature 330 (1987) 80–82.

[35] M.H. Paclet, S. Berthier, L. Kuhn, J. Garin, F. Morel, Regulation of phagocyte NADPH oxidase activity: identification of two cytochrome b558 activation states, FASEB J. 21 (2007) 1244–1255.

[36] R. Foyouzi-Youssefi, F. Petersson, D.P. Lew, K.H. Krause, O. Nusse, Chemoattractant-induced respiratory burst: increases in cytosolic Ca^{2+} concentrations are essential and synergize with a kinetically distinct second signal, Biochem. J. 322 (Pt 3) (1997) 709–718.

[37] S. Bréchard, C. Melchior, S. Plançon, V. Schenten, E.J. Tschirhart, Store-operated Ca^{2+} channels formed by TRPC1, TRPC6 and Orai1 and non-store-operated channels formed by TRPC3 are involved in the regulation of NADPH oxidase in HL-60 granulocytes, Cell Calcium 44 (2008) 492–506.

[38] F. Guignard, J. Mauel, M. Markert, Phosphorylation of myeloid-related proteins MRP-14 and MRP-8 during human neutrophil activation, Eur. J. Biochem. 241 (1996) 265–271.

[39] C. van den Bos, J. Roth, H.G. Koch, M. Hartmann, C. Sorg, Phosphorylation of MRP14, an S100 protein expressed during monocytic differentiation, modulates Ca(2+)-dependent translocation from cytoplasm to membranes and cytoskeleton, J. Immunol. 156 (1996) 1247–1254.

[40] C. Kerkhoff, I. Eue, C. Sorg, The regulatory role of MRP8 (S100A8) and MRP14 (S100A9) in the transendothelial migration of human leukocytes, Pathobiology 67 (1999) 230–232.

[41] T. Smani, S.I. Zakharov, E. Leno, P. Csutora, E.S. Trepakova, V.M. Bolotina, Ca2+-independent phospholipase A2 is a novel determinant of store-operated Ca2+ entry, J. Biol. Chem. 278 (2003) 11909–11915.

[42] M. Flourakis, F. Van Coppenolle, V. Lehen'kyi, B. Beck, R. Skryma, N. Prevarskaya, Passive calcium leak via translocon is a first step for iPLA2-pathway regulated store operated channels activation, FASEB J. 20 (2006) 1215–1217.

[43] K. Itagaki, C.J. Hauser, Sphingosine 1-phosphate, a diffusible calcium influx factor mediating store-operated calcium entry, J. Biol. Chem. 278 (2003) 27540–27547.